ECS Transactions, 85 (13) 559-564 (2018)
10.1149/08513.0559ecst ©The Electrochemical Society

Charge Transfer within Metal-Organic Frameworks: The Role of Polar Node in the Electrocatalysis and Charge Storage

J. Yu, A. Van Wyk, T. Smith, and P. Deria
Department of Chemistry and Biochemistry, Southern Illinois University, 1245 Lincoln Drive, Carbondale, IL 62901

Metal-organic frameworks (MOFs) assembled from the photo and redox-active building blocks such as porphyrins and pyrenes, as well as numerous post-synthesis processes that enable incorporation of required chemical functionality within the pores have signified these crystalline molecular assemblies as emerging class of compositions for energy conversion, and storage systems. Electrochemical energy conversion and storage applications require efficient charge transport process within the frameworks. While it is known that a large difference in the redox potentials between the linkers and metal-oxo nodes enforces a hopping type charge transport processes, the impact of the metal-oxo nodes is merely speculative. Part of the reason being the involvement of counter ion that must follow the charge hopping process. This work highlights impacts of Zr_6^{IV}-oxo node in the electronic structure of the framework compositions and the role it plays in the electrocatalytic process.

Metal-organic frameworks (MOFs) represents a crystalline molecular assembly of redox-active species and are emerging material in the energy field due to its inherent porosity that can provide high catalytically active surface area and substrate accessibility. Perhaps the most critical benefit of these framework compositions in energy conversion and storage systems is the high surface concentration they provide when posted on an active electrode.[1] While their precisely assembled photo-active linkers can facilitate efficient energy transfer to be considered as a great platform material for light harvesting utility,[2-4] the photon energy conversion and storage need efficient electron transfer process within the frameworks. Considering large energy mismatch between the metal-oxo nodes and the redox active linkers, counter ion migration is required in an electrochemically studied charge transfer reaction in these porous compositions. This leads to unique situations including a slower kinetic and selective redox reaction [i.e. a modified self-exchange reaction: $L^+—PF_6^- + L^0 \rightarrow L^0—PF_6^- + L^+$].[5] Thus it is important to understand if the metal-oxo nodes, in these framework compositions, alter the electronic properties of the linker assemblies and if they play a role in the charge transfer dynamics. This paper will discuss how the charge-transfer process is inherently different within the pores and that the metal-oxo node can play a critical role in the CT kinetics without the involvement of the counter ions.

Experimental

Materials: Reagent grade solvents including DMF and acetone were purchased from Fisher Scientific whereas the analytical grade solvents used for physical measurements were obtained from Sigma-Aldrich. Two Zr_6^{IV}-oxo based framework compositions, known as UiO-66 and NU-1000 were prepared according to literature procedure.[6, 7] Microcrystalline NU-1000 samples decorated with ferrocene carboxylate, **Fc@NU-1000**, was realized *via* SALI-based node functionalization technique;[8-11] in brief, solid NU-1000 (60 mg; 0.023 mmol) was reacted with desired amount of Fc-COOH (2 mM) solution in DMF in 10 mL

vials at 60 °C for 24 h. The resulting solid sample was centrifuged and washed with fresh DMF (5×) followed by acetone (4×), and finally dried in a vacuum desiccator. The loadings of Fc-COO^- at the node were determined via SEM-EDS elemental analysis.

Measurements: cyclic voltammograms were recorded on an Autolab 128N potentiostat using standard three electrode setup that employs a GC or FTO working, an Ag/AgCl (3M KCl) reference, and a Pt counter electrode, in 0.1 M DMF solution of $TBAPF_6$ with a scan rate of 50 mV/s. The UV-vis absorptive spectra for the solid samples were recorded as diffused reflectance spectra using a JASCO V-670 UV-vis-NIR spectrophotometer equipped with a 60 mm $BaSO_4$ –coated integrating sphere. Steady-State emission spectra were recorded at room temperature using Edinburgh FS5 spectrofluorimeter in a front-face configuration where the solid samples were packed inside quartz capillary tube that is charged with nitrogen or respective solvents. The absolute quantum yields were measured using a 150 mm integrating sphere. Fluorescence lifetime emission decay profiles were recorded using an Edinburgh Lifespec II Picosecond Time-Correlated Single Photon Counting spectrophotometer (Hamamatsu H10720-01 detector; 405 nm picosecond pulsed diode laser as TCSPC source; IRF 180p ps). Instrumental control, kinetic data collection, processing, and fitting were performed using the F980 software.

Result and Discussions

Since an electrochemical energy conversion and storage system has to operate over many cycles, the corresponding working composition is required to be robust. Framework compositions based on Zr_6^{IV}-oxo nodes are hydrolytically and mechanically robust; due to a strong Zr^{IV}-carboxylate bond, these structures are compatible to a wide range of dielectric media including aqueous acid under prolong exposure that is typically required for electrocatalytic conditions.[12-15] Literature reports indicate that the Zr_6^{IV}-oxo node may have a negligible impact of on the electronic properties of the linker assembly. This is mainly due to a large (> 4.5 eV) bandgap for the Zr_6^{IV}-oxo cluster, whose DOS lies >1 eV relative to a large band-gap linker such as benzene dicarboxylic acid (BDC).[16]

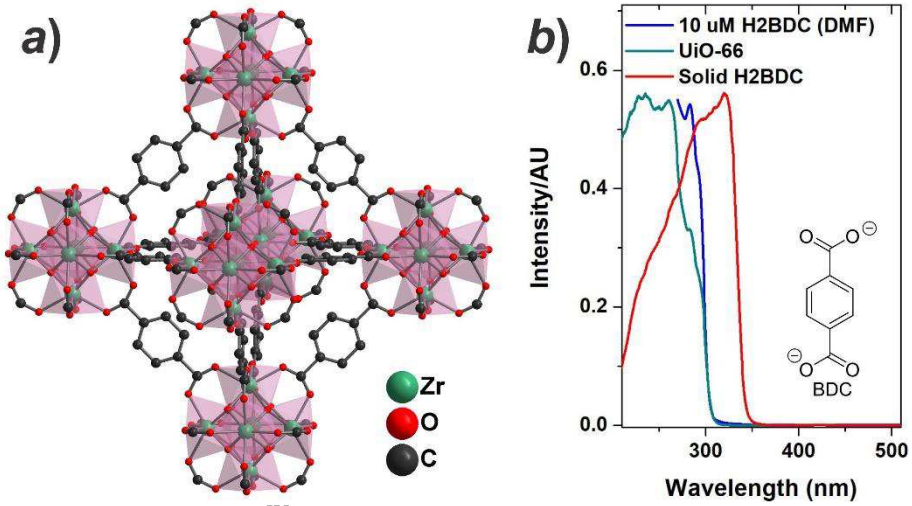

Figure 1. (a) Structure of Zr_6^{IV}-oxo based framework material UiO-66. (b) Electronic spectra showing the band-edge difference of BDC linker in Zr_6-oxo node bound form as UiO-66 (dark cyan) and free as (i) 0.01 mM solution in DMF (blue) and (ii) solid (red).

Thus, it can be expected that even for a framework material composed with a large band-gap linker, the optical properties of UiO-66 is defined by a ligand -centered π- π* transition generating optical spectra that is identical to that of the free H_2BDC linker in

DMF solvent (10 μM; **Figure 1**).[17, 18] It should be noted in this context that the interchromophoric interactions of the linker molecule in their stacked solid form render a sizable redshift (~0.45 eV).

DFT computational[19] studies suggest that the commonly used π-conjugated linkers will align their respective frontiers orbitals/band energy levels such that they do not mix significantly (Type-I). To further understand this point we performed electrochemical studies of another Zr_6^{IV}-oxo node-based framework material NU-1000 that is composed of a redox active 1,3,6,8-tetrakis(*p*-benzoicacid) pyrene (H_4TBAPy).

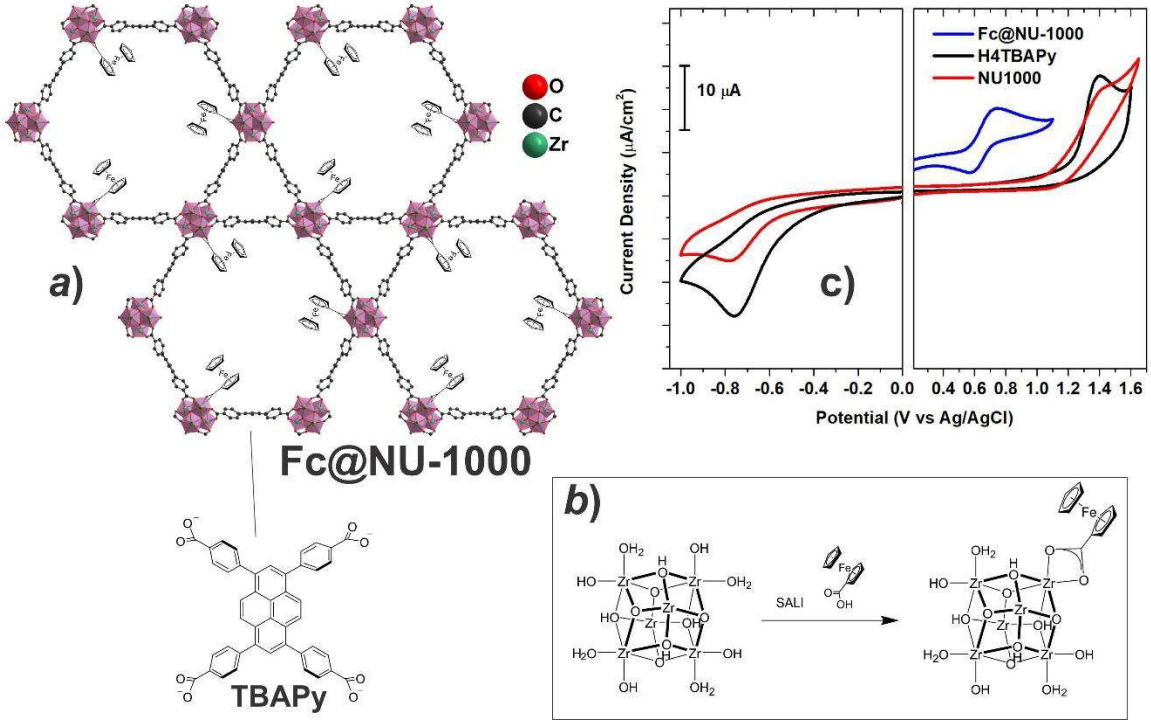

*Figure 2. (a) Structure of Fc-decorated NU-1000 composition. (b) Installation of the ferrocene-carboxylate at the Zr-oxo node via Solvent-Assisted Ligand Incorporation (SALI) method. (c) Cyclic voltammograms of H_4TBAPy, NU-1000, and **Fc@NU- 1000**.*

As expected, the electrochemical data suggest that the binding of the TBAPy linkers with the Zr_6^{IV}-oxo node does not alter its electronic energy levels relative to a free H_4TBAPy in DMF solution. Thus, in these neutral compositions, it is fair to conclude that Zr_6^{IV}-oxo node play a charge-balancing role beside constructing the robust frameworks. It is important to note that the energy level alignment between a Ti^{IV} -based node and a π-conjugated linker can be different due to a lower lying LUMO or conduction band of the metal node that can promote an electronic coupling.[19]

With these spectroscopic and electrochemical data clearly highlight a large frontier energy mismatch between a Zr_6^{IV}-oxo node and a redox active linker, charge transport within such materials will only commence via a self-exchange type hopping mechanism. However, the involvement of counterions can potentially alter the charge-transfer (CT) kinetics by modifying the driving force, and adding diffusion related thermodynamic parameters. Thus, to understand what role a polar Zr_6^{IV}-oxo node can play during a charge transfer reaction, the involvement of the counter ions was eliminated *via* installing a redox partner close to the TBAPy moieties within the frameworks. In this regard, the Zr_6^{IV}-oxo node play as the anchoring point for a complimentary redox species such as ferrocene[5]

using a SALI (Solvent-Assisted Ligand Incorporation) -based node functionalization technique to generate **Fc@NU-1000** (Figure 2).[10, 20, 21]

To figure out if these apparently polar metal-oxo clusters hosting several hydroxyl and aqua ligand protruding to the pores at a close proximity of the TBAPy linkers can play any role other than being electronically inert, ferrocene carboxylates were installed at the Zr_6^{IV}-oxo node via SALI; DFT-optimized structure of **Fc@NU-1000** suggests that the installed ferrocene moiety is rigidly anchored at a close proximity of the Zr-oxo node (with a shortest Fc-to- TBAPy distance of 9.7 Å). Electrochemical data (Figure 2 c) suggests that the node-anchored Fc moieties are electrochemically accessible at +0.7V Fc/Fc^+ potential, where the TBAPy linkers in pristine NU-1000 can be electronically oxidized at +1.4 V. with this energy level alignment, we expect that the Fc moiety can efficiently quench the TBAPy based emission from photoexcited NU-1000* forming a **[NU-1000]$^{\bullet-}$/Fc$^+$** CT complex

CT rate constants as function of solvent dielectrics were determined via analyzing the fluorescence quenching experimental data using equation (1):

$$\frac{\Phi_0}{\Phi_s} = 1 + \tau_0 k_e \qquad (1)$$

where Φ_0 and τ_0 are the intrinsic quantum yield and lifetime without quenchers, respectively; Φ_s is the saturated fluorescence quantum yield; and k_e is the CT (quenching) rate.

Under the assumption of static fluorescence quenching, the decay of [NU-1000]* in the Fc@NU-1000 sample can be described as two competitive processes, where the photo-excited S_1 state depletes *via* an $S_1 \rightarrow S_0$ decay (emission) and CT reaction with ferrocene (quenching).[22] To find out a quantum yield (QY) at the saturation (maximum) quenching condition, Fc loading was varied from zero to a maximum of 0.353 per TBAPy linker. As shown in Figure 3, the absolute QY, emissive lifetime quickly diminish with increasing ferrocene loading and plateaus at an Fc/TBAPy ratio of ~0.06.

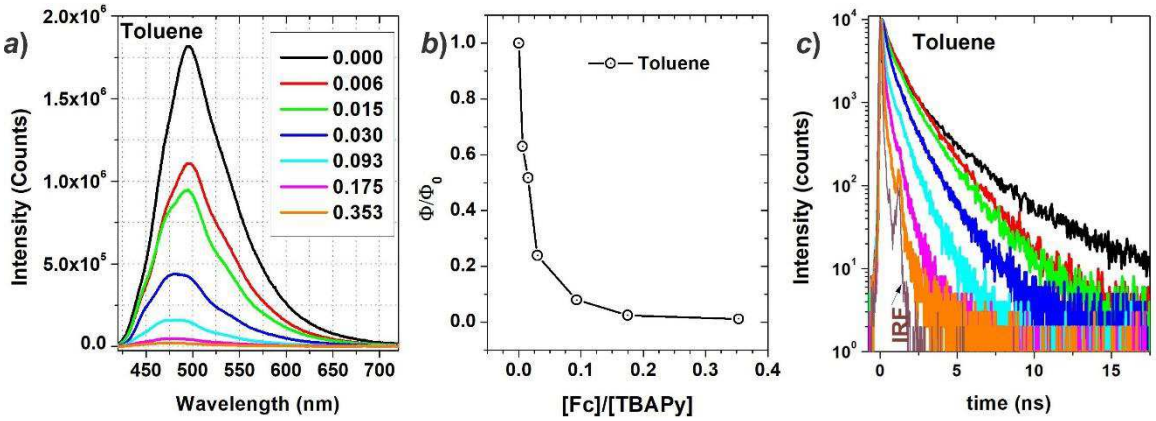

Figure 3. Emission quenching as a function of Fc/TBAPy ratio: (a) reduction of QY, (b) quenching efficiency, and (c) faster decay (in Toluene solvent).

The CT lifetimes extracted from the emission quenching experiments provide a rate constant of 7.5×10^{10} s^{-1} was found in toluene solvent which falls within the range of rate constant expected for $r_{DA} \simeq 10$ Å.[23, 24] However, a solvent dielectric dependent rate constant rendered a surprising trend: with the variation of ϵ_s from 1-9 (air-trifluorotoluene) the CT rate constant remained essentially unchanged. Such behavior can be expected for a system possessing high total reorganization energy that is similar to the ΔG^0. While the later value obtained from the electrochemical data to be -0.74 to -1.1 eV (in high to low polar solvent),

the total reorganization energy in low dielectric media (negligible λ_s) is contributed only by the internal vibrational component (λ_i = 0.42 eV). This disparity suggests the existence of a polar component that contributes to the λ_i value. Considering the fact that the ferrocene moiety is deeply buried within the Zr_6^{IV}-oxo node that host hydroxyl and aqua ligands can play a role reminiscent of a polar solvent. Note that the frontier molecular orbital for the TBAPy linker (especially the LUMO for the anion) also extends to these Zr_6^{IV}-oxo nodes through the bridging phenyl rings, which also should require some polarization to stabilize the charged species.

Conclusions

Overall, this study shows that the Zr_6^{IV}-oxo nodes do not alter the electronic property (HOMO/LUMO energy levels) for the bound linkers in the framework composition, which may stem from a significant mismatch of the frontier energy levels of the respective component owing to a large band-gap of the cluster. However, these polar Zr_6^{IV}-oxo clusters host hydroxyl and aqua ligands which may require a sizable reorganization energy for linker/ligands that possess charge-density in the close proximity of the node to slow down the charge-transport rate within such framework materials.

Acknowledgments

We thank SIUC and ACERC for the startup and a partial support through Energy Boost Seed Grant, respectively. P.D. acknowledges Ralph E. Powe Junior Faculty Enhancement Award, administered by ORAU. A.V.W. acknowledges NSF-REU fellowship (DMR1461255).

References

1. I. Hod, M. D. Sampson, P. Deria, C. P. Kubiak, O. K. Farha and J. T. Hupp, *ACS Catalysis*, **5**(11), 6302 (2015).
2. H.-J. Son, S. Jin, S. Patwardhan, S. J. Wezenberg, N. C. Jeong, M. So, C. E. Wilmer, A. A. Sarjeant, G. C. Schatz, R. Q. Snurr, O. K. Farha, G. P. Wiederrecht and J. T. Hupp, *J. Am. Chem. Soc.*, **135**(2), 862 (2013).
3. P. Deria, J. Yu, R. P. Balaraman, J. Mashni and S. N. White, *Chem. Commun.*, **52**(88), 13031 (2016).
4. C. Wang, Z. Xie, K. E. deKrafft and W. Lin, *J. Am. Chem. Soc.*, **133**(34), 13445 (2011).
5. S. Patwardhan and G. C. Schatz, *J. Phys. Chem. C*, **119**(43), 24238 (2015).
6. T. C. Wang, N. A. Vermeulen, I. S. Kim, A. B. F. Martinson, J. F. Stoddart, J. T. Hupp and O. K. Farha, *Nature Protocols*, **11**, 149 (2015).
7. M. J. Katz, Z. J. Brown, Y. J. Colon, P. W. Siu, K. A. Scheidt, R. Q. Snurr, J. T. Hupp and O. K. Farha, *Chem. Commun.*, **49**(82), 9449 (2013).
8. P. Deria, J. E. Mondloch, E. Tylianakis, P. Ghosh, W. Bury, R. Q. Snurr, J. T. Hupp and O. K. Farha, *J. Am. Chem. Soc.*, **135**, 16801 (2013).
9. P. Deria, W. Bury, I. Hod, C.-W. Kung, O. Karagiaridi, J. T. Hupp and O. K. Farha, *Inorg. Chem.*, **54**, 2185 (2015).
10. P. Deria, W. Bury, J. T. Hupp and O. K. Farha, *Chem. Commun.*, **50**, 1965 (2014).
11. P. Deria, Y. G. Chung, R. Q. Snurr, J. T. Hupp and O. K. Farha, *Chem. Sci.*, **6**, 5172 (2015).
12. I. Hod, P. Deria, W. Bury, J. E. Mondloch, C.-W. Kung, M. So, M. D. Sampson, A. W. Peters, C. P. Kubiak, O. K. Farha and J. T. Hupp, *Nature Commun.*, **6**, 8304 (2015).

13. I. Hod, M. D. Sampson, P. Deria, C. P. Kubiak, O. K. Farha and J. T. Hupp, *ACS Catalysis*, **5**, 6302 (2015).
14. S. R. Ahrenholtz, C. C. Epley and A. J. Morris, *J. Am. Chem. Soc.*, **136**, 2464 (2014).
15. P. M. Usov, S. R. Ahrenholtz, W. A. Maza, B. Stratakes, C. C. Epley, M. C. Kessinger, J. Zhu and A. J. Morris, *J. Mater, Chem. A*, **4**, 16818 (2016).
16. A. De Vos, K. Hendrickx, P. Van Der Voort, V. Van Speybroeck and K. Lejaeghere, *Chem. Mater.*, **29**, 3006 (2017).
17. J. He, J. Wang , Y. Chen, J. Zhang, D. Duan, Y. Wang and Z. Yan, *Chem. Commun.*, **50**, 7063 (2014).
18. K. Hendrickx, D. E. P. Vanpoucke, K. Leus, K. Lejaeghere, A. Van Yperen-De Deyne, V. Van Speybroeck, P. Van Der Voort and K. Hemelsoet, *Inorg. Chem.*, **54**, 10701 (2015).
19. M. A. Nasalevich, C. H. Hendon, J. G. Santaclara, K. Svane, B. van der Linden, S. L. Veber, M. V. Fedin, A. J. Houtepen, M. A. van der Veen, F. Kapteijn, A. Walsh and J. Gascon, *Scientific Reports*, **6**, 23676 (2016).
20. I. Hod, W. Bury, D. M. Gardner, P. Deria, V. Roznyatovskiy, M. R. Wasielewski, O. K. Farha and J. T. Hupp, *J. Phys. Chem. Lett.*, **6**, 586 (2015).
21. P. R. McGonigal, P. Deria, I. Hod, P. Z. Moghadam, A.-J. Avestro, N. E. Horwitz, I. C. Gibbs-Hall, A. K. Blackburn, D. Chen, Y. Y. Botros, M. R. Wasielewski, R. Q. Snurr, J. T. Hupp, O. K. Farha and J. F. Stoddart, *Proc. Natl. Acad. Sci. U.S.A.*, **112**, 11161 (2016).
22. H.-J. Son, S. Jin, S. Patwardhan, S. J. Wezenberg, N. C. Jeong, M. So, C. E. Wilmer, A. A. Sarjeant, G. C. Schatz, R. Q. Snurr, O. K. Farha, G. P. Wiederrecht and J. T. Hupp, *J. Am. Chem. Soc.*, **135**, 862 (2013).
23. H. B. Gray and J. Winkler, R., *Proc. Natl. Acad. Sci. U.S.A.*, **102**, 3534 (2005).
24. J. Winkler, R. and H. B. Gray, *J. Am. Chem. Soc.*, **136**, 2930 (2014).